Comparative Analysis of Different Control Techniques for the Both-Sides Retrodirective Beamforming System

Joselito Ramento Jr.
Electrical and Electronics Engineering Institute
University of the Philippines - Diliman
Quezon City, Philippines
joselito.jr.ramento@eee.upd.edu.ph

Charleston Dale Ambatali
Electrical and Electronics Engineering Institute
University of the Philippines - Diliman
Quezon City, Philippines
charleston.ambatali@eee.upd.edu.ph

***Abstract*—The both-sides retrodirective array is a beamforming technique that achieves maximum power delivered from a sending node to a receiving node. It can be used in wireless power transfer and wireless communications. The system can achieve fast beam convergence and maximum transfer efficiency operation for any given channel setting without explicit channel estimation. However, the system must maintain marginal stability to continuously operate at this optimal condition, which requires proper transmit gain settings on both arrays. In this paper, we explored two control schemes to drive the system to this marginally stable state, one based on linear quadratic control and another on fuzzy logic control. Both controllers were designed and tested in time-domain simulations to determine their performance in different channel settings. Simulation results show that the proposed system was more consistent and faster in achieving the maximum efficiency condition when compared to other existing beam focusing methods asserting that the proposed control schemes can realize the advantages of both-sides retrodirective array as a beamforming system.**

***Index Terms*—beamforming, control, LQR, fuzzy logic, retrodirective arrays**

I. Introduction

Beamforming is a solution in wireless communications to focus a beam from an antenna array in a direction to an intended receiver. A successful beam formation and steering avoids the multipath problem, increasing the coherence bandwidth of the system and consequently, its communication capacity [1]. As the antenna arrays grow larger with respect to their wavelength of operation, the closer they operate in the Fresnel zone. It is in this zone where power can be delivered efficiently from a transmitting node to a receiving node [2], [3]. However, beam focusing becomes slower as the antenna size increases.

Formulation and analysis of beamforming in the Fresnel zone becomes complicated as system approximations in the reactive near-field and far-field regions cannot be exploited. Therefore, a new paradigm for analysis is required, and in this paper, the wireless channel was modeled using S-parameters [4]. According to this framework, by modeling the channel as an N-port network, where N is the number of antenna elements in both generator and receiver arrays, the maximum transfer efficiency, $\eta_{\max}$, for any given channel condition is dictated by the following equations,

$$\eta = \frac{\mathbf{v_{2f}}^H \left(\mathbf{S_{21}}^* \mathbf{S_{21}}^T\right) \mathbf{v_{2f}}}{\mathbf{v_{2f}}^H \mathbf{v_{2f}}} \tag{1}$$

$$\eta_{\max} = \max\left(\text{eig}\{\mathbf{S_{21}}^* \mathbf{S_{21}}^T\}\right) = \xi_{\max} \tag{2}$$

where $\mathbf{A}^*$, $\mathbf{A}^T$, $\mathbf{A}^H$ are the matrix conjugate, transpose, and Hermitian transpose of $\mathbf{A}$, and ξ is an eigenvalue of $\mathbf{S_{21}}^* \mathbf{S_{21}}^T$. This also assumes a reciprocal channel and perfect matching and decoupling networks within each array. Equation (1) also reveals the existence of several input combinations corresponding to other specific operating efficiencies, and the maximum can be achieved by using a linear combination of eigenvector/s corresponding to $\xi_{\max}$.

Analyzing existing beam focusing methods using this framework reveals a tradeoff between system settling time and transfer efficiency. Solutions that offer fast settling time [5], [6] have been found to operate at suboptimal efficiencies since the optimal input combination cannot be generated consistently, while systems that can do so [7] require additional computational overhead, hence settles at a slower rate. However, a novel theoretical scheme known as the both-sides retrodirective array was found to achieve both fast settling time and maximum efficiency operation [3], [8]. This performance, nonetheless, requires the system to be maintained at marginal stability. Therefore, a proper control system must be designed to fully realize its potential.

II. Dynamic Beam Focusing Methods

A. Existing Methods

Several beam focusing methods have been proposed in the literature to maximize power delivered over long distances. These methods have been roughly divided into three categories [9]. The first class uses position sensors to optimize beam steering solely through phase control [5]. The second class employs retrodirective capabilities on one of the arrays to train a pilot signal that could track the position of the other array using passive phase control without additional computational overhead or explicit location inputs [6]. While these first two classes of systems can achieve fast convergence, the lack of knowledge about the channel or its integration into the

979-8-3315-6946-4/25/$31.00 ©2025 IEEE

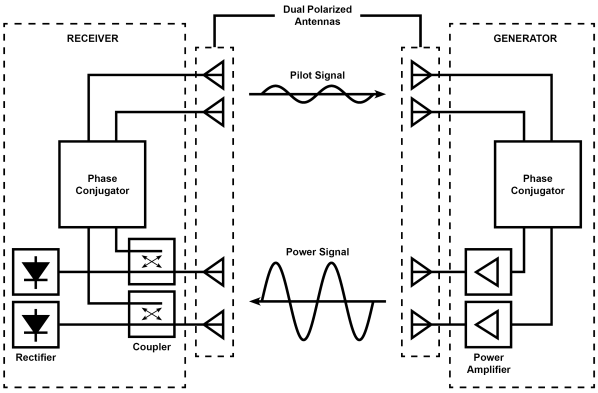

Fig. 1: General operation of the BS-RDAA system

beamforming process limits their operating efficiencies due to suboptimal input combinations as previously mentioned.

The last class of methods uses telemetry to actively send relevant data for explicit channel estimation or beamforming using iterative optimization algorithms [7]. These methods can theoretically maintain maximum power transfer operation as enough channel characterization can be integrated into the beamforming process. However, the additional computational overhead results in slow system convergence, reducing overall efficiency and posing problems in dynamic channel settings.

B. Both-Sides Retrodirective Antenna Array System

A novel approach for automated beam focusing called the both-sides retrodirective antenna array (BS-RDAA) system employs retrodirective capabilities on the receiver and generator arrays, creating a loop feedback that allows both to track each other's position via phase and amplitude control [8]. The general operation of the BS-RDAA system is illustrated in Fig. 1.

Previous studies had already highlighted the capability of BS-RDAA system to automatically generate the optimal beamform that can minimize the power lost to free space for a given channel condition with relatively fast settling time. [3], [8], [9]. However, maintaining this maximum efficiency operation necessitates driving the system to marginal stability, which requires the transmit gain at both generator and receiver arrays to follow the equation

$$|LG| = \frac{1}{\xi_{\max}} = \frac{1}{\eta_{\max}} \tag{3}$$

where L and G are the transmit gain at the receiver and generator arrays, respectively [3]. These findings also reveal that, at the minimum, the BS-RDAA system only requires manual gain control as the phase is already automatically adjusted through the arrays' retrodirective operation.

C. Previous BS-RDAA Control Implementation

As discussed, determining and maintaining proper gain settings is crucial for the optimal operation of the BS-RDAA system. While this can be done by fully characterizing or estimating the current channel parameters and subsequently tuning the gains, this method can introduce significant computational overhead that could slow down system settling time, which is very important in practical, time-varying channel conditions. As such, automatic gain determination without prior knowledge of the channel is important to maximize the capabilities of the BS-RDAA system. Given this restriction on the desired operation, formulating a system model based on the combinations of voltage signals, or beam modes comprising the pilot and power signals, hence as a multiple input, multiple output (MIMO) system, is currently difficult, as the effects of the channel on the individual signal combinations cannot be determined beforehand.

Only a single study had explored the BS-RDAA control given this operational restriction, proposing a classical control theory perspective to achieve the functionality [9]. An equivalent single input, single output (SISO) model was formulated using the total power flowing within the system. From the steady-state dynamics equation of the BS-RDAA [3],

$$\lim_{t\to\infty} \mathbf{v_{2f}}(t) = (LG^*\xi_{\max})^{t/t_p}\mathbf{v_{i,\max}} \tag{4}$$

where t_p is the total loop propagation time and $\mathbf{v_{i,\max}}$ is the optimal input combination or beam mode generated at steady state, the following SISO model was calculated with the received power, $P = \mathbf{v_{1b}}^H\mathbf{v_{1b}}/Z_0$, where Z_0 is the matched impedance assumed to be equal for all ports and $\mathbf{v_{1b}} = \mathbf{S_{21}}^T\mathbf{v_{2f}}$, and P_0 as the starting power [9],

$$P(t) = P_0|\xi_{\max}LG|^{t/t_p} \tag{5}$$

This was then linearized in the logarithmic domain to yield the following,

$$p(t) = u\frac{t}{t_p} + g\frac{t}{t_p} + p_0 \tag{6}$$

where $p(t)$ is the power received at the time t and p_0 is the initial power of the system, both in decibel-Watts (dBW), while $u = 20\log|L|$ and $g = 20\log|\xi_{\max}G|$ are the system gains in decibels (dB). With this, u was set as the (actuator) input to the system and g as an external disturbance.

With this model, a classical integral-proportional (IP) controller was designed in the previous study to drive the system to marginal stability [9]. Results showed that the system consistently operated to within 2% of the maximum efficiency in a time-varying channel while maintaining a constant power output at the receiver. However, the controller exhibited undesirable transient response characteristics such as overshooting and oscillations, esp. in relatively low efficiency channel settings, which could potentially damage devices.

Therefore, this paper seeks to address this gap in the literature and the limitations identified in the previous controller implementation. A linear quadratic controller is proposed to directly minimize undesirable transient response characteristics and to consider the limitations of practical control devices, e.g. saturation of variable attenuators, while the feasibility of the fuzzy logic control is explored given its flexibility with systems that have relatively inaccurate mathematical models. The performance of the controllers, both in static and dynamic channel conditions, was evaluated using time-domain simulations and compared to other existing dynamic beam focusing methods.

III. System Model and Controller Design

A. System Model Testbed

The system model used as a testbed for each controller was a recreation of the MATLAB Simulink model of the BS-RDAA developed in a previous study [9]. In addition, the same S-parameter data to emulate the same dynamic channel conditions was used to facilitate straightforward performance comparison of controllers developed for this project and previous methods.

The system model used a 4-element patch antenna array for the generator and another 4-element patch antenna array for the receiver, resulting in an 8-port network model for the channel. In addition, since a reciprocal channel was assumed and an ideal case with $\mathbf{S_{11}} = \mathbf{S_{22}} = \mathbf{0_4}$, only the $\mathbf{S_{12}}$ and $\mathbf{S_{12}}^T$ was used. Each S-matrix entry was interpreted as a combination of delay and amplitude scaling. The system was also set to operate at $f_0 = 2.4$GHz.

Signal conjugation was achieved using a superheterodyne architecture, with two mixers with $1.4f_0$ and $0.6f_0$ local oscillators and a pair of 2nd-order Butterworth bandpass filters with Q-factor of 10. The linear gain at the generator was fixed to 100, with output saturation limits of ± 100. The gain (attenuator) block at the receiver was set with limits of -3dB and -43dB to model a practical voltage variable attenuator. The logarithmic gain was then converted to linear domain before being multiplied to the output of the receiver conjugator blocks. Finally, moving average blocks were used to calculate instantaneous power, and the transfer efficiency was calculated. Each controller was implemented within the receiver antenna array subsystem for testing.

B. Linear Quadratic Controller

For the design of the linear quadratic controller (LQC) [10], a state-space representation of the system dynamics with an additional state for output power error was first formulated. As previously discussed, the dynamics of the system can be expressed through equation 6. Taking the derivative of this simplified dynamics equation to yield a differential equation for the total power of the system and adding a state for the integral of power error with r as reference input results in the following state-space equations, ignoring the effects of g for simplicity,

$$\begin{aligned} \begin{bmatrix} \dot{p} \\ \dot{e} \end{bmatrix} &= \begin{bmatrix} 0 & 0 \\ -1 & 0 \end{bmatrix} \begin{bmatrix} p \\ e \end{bmatrix} + \begin{bmatrix} 1/t_p \\ 0 \end{bmatrix} \begin{bmatrix} u \end{bmatrix} + \begin{bmatrix} 0 \\ 1 \end{bmatrix} \begin{bmatrix} r \end{bmatrix} \\ y &= p \end{aligned} \tag{7}$$

The built-in lqr function in MATLAB was then used on state equation (7) to determine the gain matrix $\mathbf{K}$ for the following control law,

$$u = -\mathbf{K} \begin{bmatrix} p \\ e \end{bmatrix} = -K_1 p - K_2 \int_0^t (r - p) d\tau \tag{8}$$

Shown below are the costs used for the LQR calculation and the resulting gain matrix with $t_p = 26.33$ns.

$$\mathbf{Q} = \begin{bmatrix} 1 & 0 \\ 0 & 100 \end{bmatrix}, \ \mathbf{R} = 10, \ \mathbf{K} = \begin{bmatrix} 0.3162 & -3.1623 \end{bmatrix}$$

Running the controller with these gains revealed that the integrator response was very slow. Upon testing several integrator gains, a value of $50000K_2$ was found to result in relatively fast settling times with very minimal to no transient oscillations. The new gain matrix is as follows,

$$\mathbf{K} = \begin{bmatrix} 0.3162 & -1.5811 \times 10^6 \end{bmatrix}$$

An additional bias of -50dB was also found to cancel the effects of the disturbance g during startup across a wide range of channel efficiencies. The resulting LQC is shown in Fig. 2.

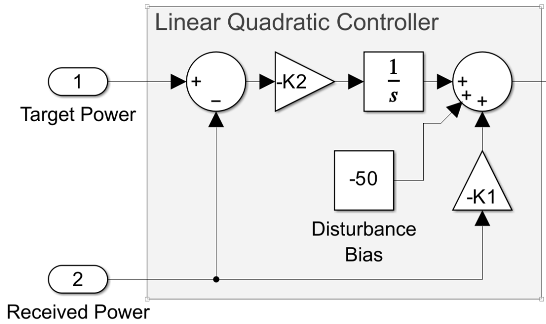

Fig. 2: Simulink flowgraph of proposed linear quadratic controller

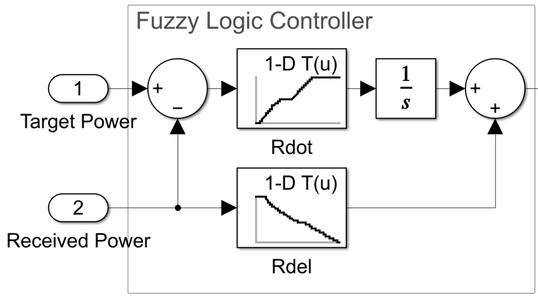

Fig. 3: Simulink flowgraph of proposed fuzzy logic controller

C. Fuzzy Logic Controller

The fuzzy logic controller (FLC) [11] was designed in MATLAB with two independent Mamdani fuzzy inference systems (FIS) with centroid rule for defuzzification. The first FIS takes in crisp power error values and outputs the rate of change of gain, $\dot{R}$, while the second FIS outputs a compensating signal, ΔR, based on the current power level at the receiver. The $\dot{R}$ output of the first FIS was fed to an integrator before being combined with the ΔR output of the second one to constitute the gain control signal at the receiver. This implementation ensures that the optimal gain can be automatically found even without explicit knowledge of the channel, as long as the controller keeps the system in marginal stability. On the other hand, the compensating signal was introduced to slow down the integrator at startup, since the system initializes with very low power levels.

The first FIS used 7 input membership functions (IMF) and 5 output membership functions (OMF) while, the second FIS used 6 IMF and 7 OMF. Each FIS was tuned by fixing the IMFs and manually adjusting the OMF placement and the rule base based on the observed response of each controller iteration. The final membership functions are illustrated in Fig. 4 while Table I shows the rulebase for each FIS.

TABLE I: Rule Base for Fuzzy Logic Controller

Error	$\dot{R}$
EHP	HP
VHP	HP
HP	HP
MP	LP
LP	0.5*LP, Z
Z	Z
N	LN

Power	ΔR
R	Z
L	VLN, LN
NL	0.7*LN, N
N	N
NH	HN
H	VHN

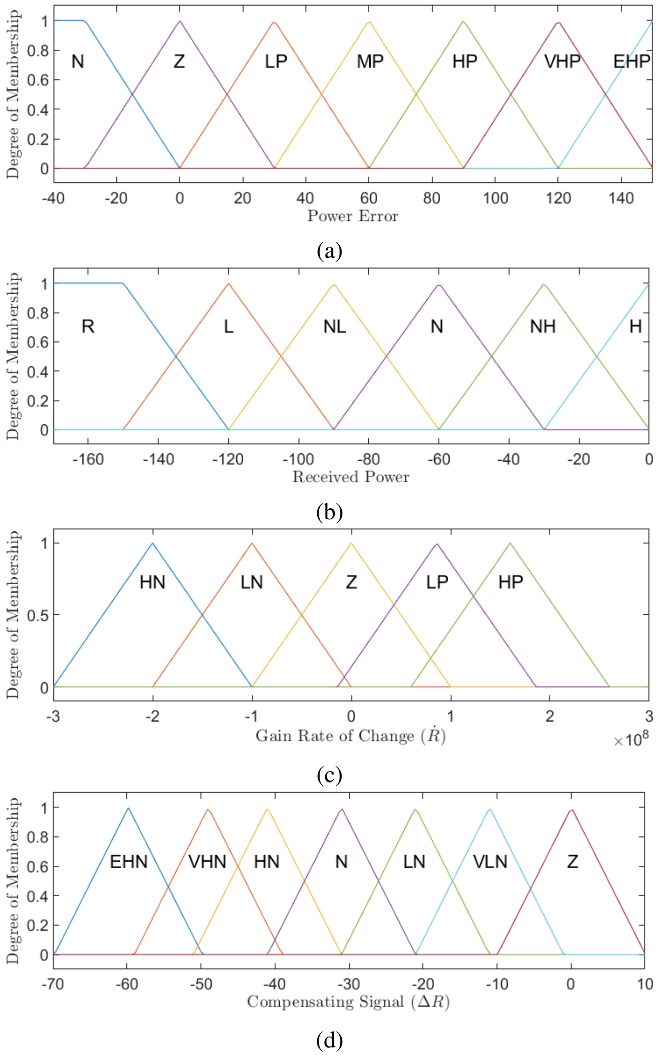

Fig. 4: Plots of (a) power error IMF, (b) received power IMF, (c) gain rate of change OMF and (d) compensating signal OMF

Each FIS was then converted into a lookup table by feeding 256 equally spaced points spanning their input range and saving the corresponding output values, simplifying the FLC operation in simulations. The final controller implementation in Simulink is shown in Fig. 3.

IV. Results and Discussion

A. Simulation in Static Conditions

To determine the transient behavior of the designed controllers, each was tested in two static channel conditions for a total duration of 1μs with a reference power of -30dBW. The first case corresponds to a channel setting with a maximum transfer efficiency of 29.95%, while the second one corresponds to an efficiency of 3.73%. These channel conditions were emulated using the corresponding set of S-parameters as dictated by equation (2). Fig. 5 shows the transient responses of each controller under the previously defined static channel settings, together with the IP controller from the previous study [9], while Table II lists the settling time, T_s, percent overshoot, percent steady-state error and integral of square error of the transient power responses.

TABLE II: Transient Power Response Characteristics

	$\eta_{\max}$	T_s (μs)	% OS	$\%\lvert e_{ss}\rvert$	ISE
LQR	3.73%	0.873	-	0.68	0.0012
	29.95%	0.271	1.20	0.06	0.00049
FLC	3.73%	0.913	-	0.84	0.0014
	29.95%	0.375	1.67	0.34	0.00054
IP	3.73%	2.048	119.2	0.44	0.0014
	29.95%	0.748	1.27	0.31	0.00040

Both controllers were successful in driving the BS-RDAA system model to marginal stability while properly tracking the reference power level. Both controllers exhibited output power overshooting in the higher efficiency case, corresponding to 0.09mW and 0.12mW overshoot above 1mW reference for LQC and FLC, respectively. However, no overshooting was observed under the lower efficiency case for both controllers. The LQC also settled to within $\delta = 0.01$ of the reference power value faster than the FLC for both cases. Both controllers were also able to track the theoretical maximum efficiencies to at most 1.14% error and the optimal gain to at most 2.52% error at steady-state.

Comparing the transient response of LQC and FLC to the previously proposed classical IP controller revealed significant improvements. Minimal to no overshooting and oscillations were observed with the new control systems, resulting in more stable operation, and faster settling times, which could improve controller adaptability in dynamic conditions. Lastly, the gain controls of the new controllers were not held at saturation values for extended periods, which could reduce stress on the attenuators used for control.

B. Simulation in Dynamic Conditions

The controllers were also tested for an extended duration with a target power of -30dBW in dynamic channel simulation corresponding to two cases, one where the generator array revolves around the receiver array, and another with an object passing through between the arrays. These cases were also emulated using their corresponding S-parameters used in the previous study [9]. Shown in Fig. 6 are the plots of the output power, efficiency, and gain control of both control systems under the two dynamic channel conditions.

Both controllers were able to maintain a near-constant output power, with less than 0.3% error or 20μW deviation. With the controllers maintaining this marginal stability condition, the system was able to track the maximum efficiency to within 1.8% error at steady-state while the gain controls were within 3.05% of the required values. These results highlighted the adaptability

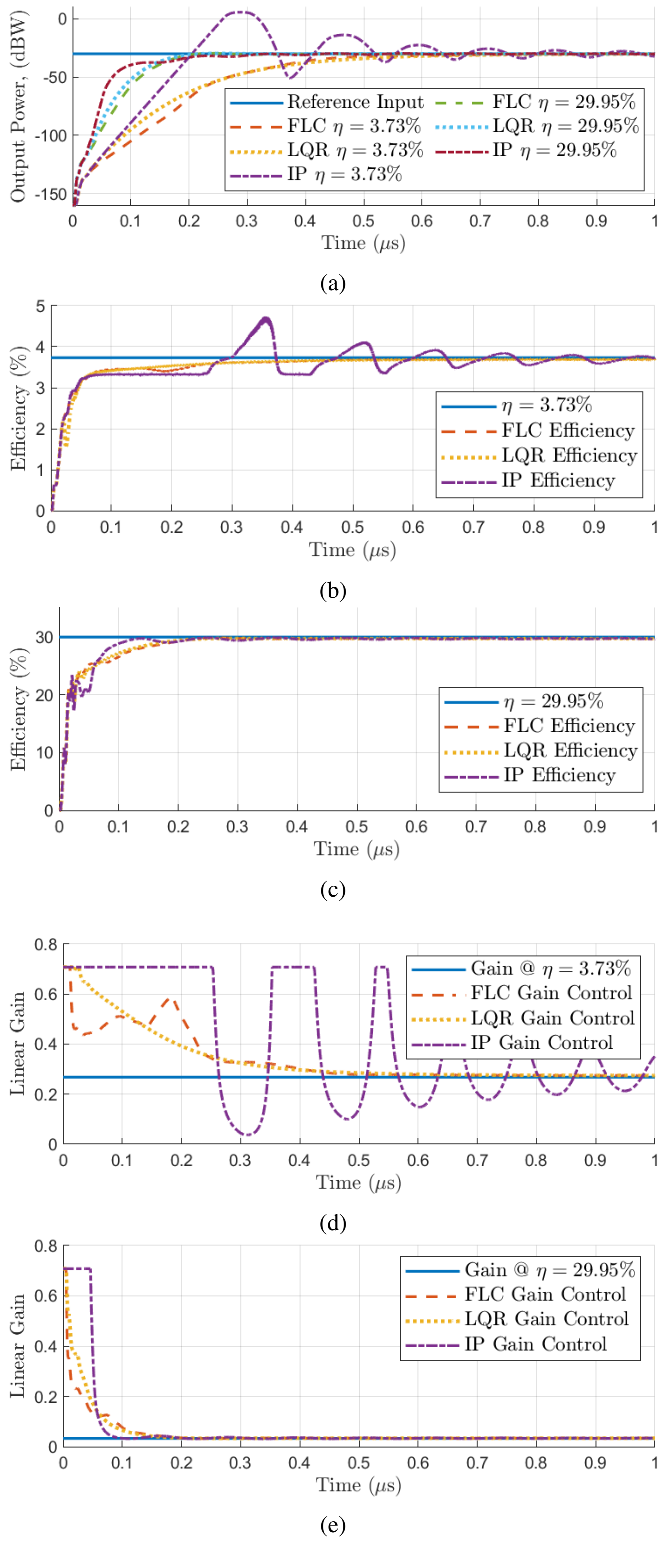

Fig. 5: Plots of (a) transient power responses, (b-c) efficiency tracking, and (d-e) gain control in high and low efficiency channel conditions

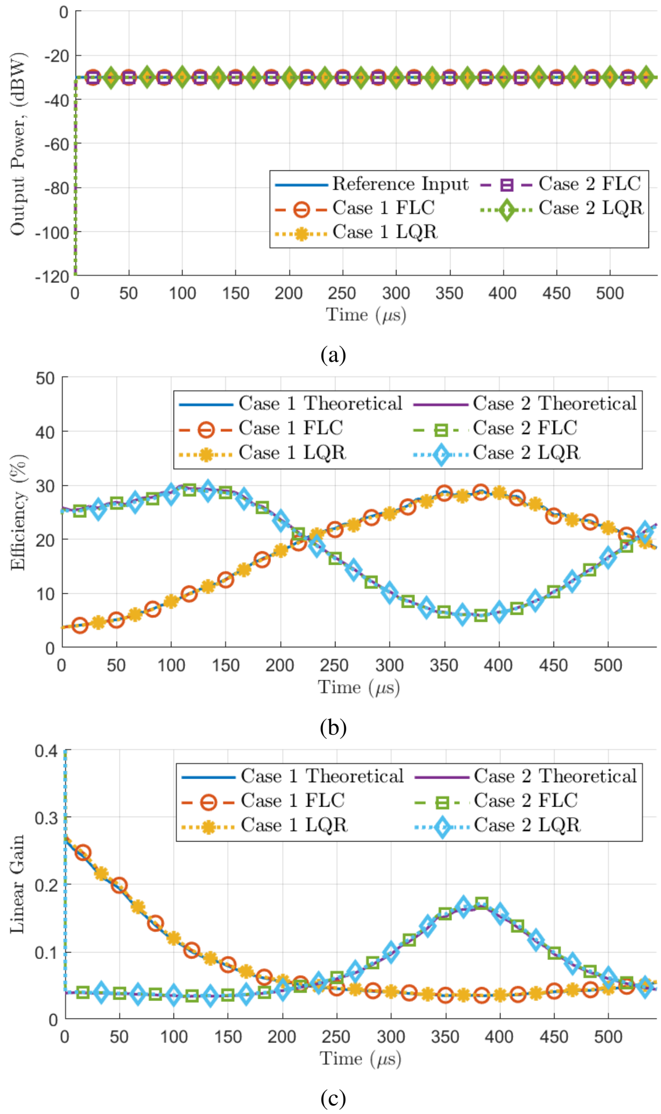

Fig. 6: Plots of (a) power tracking, (b) efficiency tracking, and (c) gain control in dynamic conditions

of the proposed controllers in time-varying channel settings, showing that maximum efficiency tracking can be achieved as long as the control system settles faster than the channel can change. On the other hand, the consistent errors in the operating efficiency and gain control may be attributed to the slowly changing channel, as the controllers implemented did not increase the overall system type with respect to the disturbance or channel efficiency as input.

C. Comparison with Other Methods

Finally, to compare the performance of each controller with some existing dynamic beam focusing methods, each one was also tested in a static channel condition corresponding to 14.45% transfer efficiency for a duration of $3\mu s$. An extended testing with the second dynamic channel case was also done. Shown in Fig. 7 are the efficiency tracking of dynamic beam focusing methods in transient static and extended dynamic conditions, using the data from the previous study [9].

The proposed controllers achieved both fast convergence and maximum efficiency operation in transient static conditions

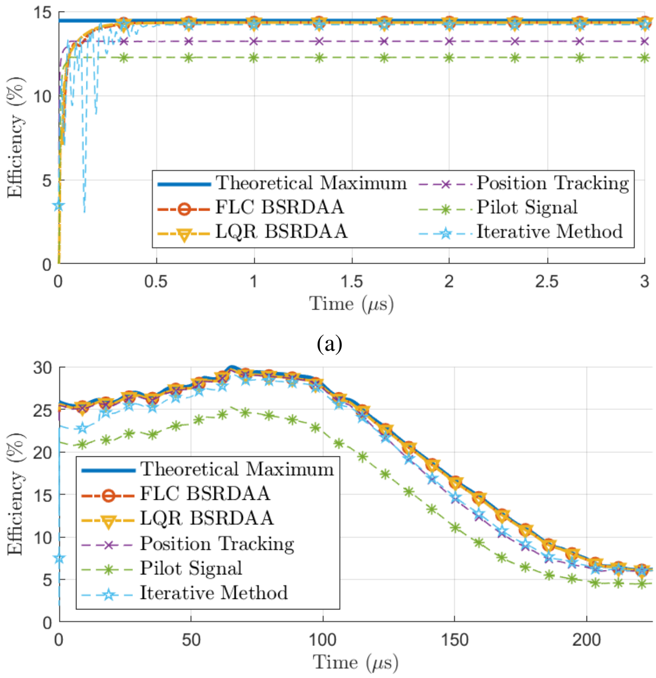

(a)

(b)

Fig. 7: Plots of efficiency tracking in (a) transient static conditions and (b) time-varying channel setting

when compared to other methods, and both were also the most consistent in maintaining the maximum efficiency condition in the simulated dynamic setting. The previously discussed trade-offs in the performance of other methods were also observed in the plots, with the ones settling the fastest having suboptimal efficiencies, while those capable of tracking the maximum efficiency have slow and unstable transient convergence, affecting their performance in dynamic settings.

V. Conclusions and Recommendations

Driving the BS-RDAA system to a marginally stable state is crucial to realizing its theoretical benefits to maximize power delivered. Upon keeping a constant power level, the BS-RDAA can track the maximum efficiency for a given channel condition without relying on complete channel estimation, offering fast system convergence that is necessary in dynamic channel conditions. To achieve this requirement, two new controllers based on linear quadratic control and fuzzy logic control were designed in this paper and were tested in time-domain simulations through MATLAB Simulink.

Results showed that both controllers were able to maintain the condition for marginal stability, tracking the required gain with at most 3.05% deviation as well as the theoretical maximum efficiency to within 1.8% error in both static and time-varying channel conditions. Results of static simulations also revealed remarkable transient performance, having minimal to no overshooting in both low and high efficiency conditions without sacrificing system settling time and increasing actuator effort. These performance observations ultimately contributed to the superior performance of the proposed system when compared to other beam focusing methods in the same channel settings, being the fastest to reach and the most consistent in maintaining maximum transfer efficiency operation. In conclusion, these results demonstrate the capacity of the proposed control schemes to realize the potential advantages of BS-RDAA in increasing the signal power at the receiver.

Building on these results and conclusions, we recommend implementing and testing the proposed control systems in hardware to gauge their feasibility outside simulations and to determine how specific non-idealities can impact their performance. It is also recommended to formulate a more accurate mathematical model of the BS-RDAA system, possibly drawing from its inherent multiple-input, multiple-output (MIMO) nature and discrete-time dynamics, as the current logarithmic SISO model substantially limits the control schemes that can be applied to the system. A more accurate model may also provide insights regarding the observed steady-state error with the operating efficiencies in time-varying settings.

Acknowledgment

We acknowledge the Office of the Chancellor of the University of the Philippines Diliman, through the Office of the Vice Chancellor for Research and Development, for funding support through the PhD Incentive Award Grant 252510 YEAR 1.

References

[1] Q. Xu, C. Jiang, Y. Han, B. Wang, and K. J. R. Liu, "Waveforming: An Overview With Beamforming," *IEEE Communications Surveys & Tutorials*, vol. 20, no. 1, pp. 132–149, 2018. [Online]. Available: https://ieeexplore.ieee.org/abstract/document/8030327

[2] V. R. Gowda, O. Yurduseven, G. Lipworth, T. Zupan, M. S. Reynolds, and D. R. Smith, "Wireless power transfer in the radiative near field," *IEEE Antennas and Wireless Propagation Letters*, vol. 15, pp. 1865–1868, 2016.

[3] C. D. M. Ambatali and S. Nakasuka, "Characterizing the dynamic behavior of a both-sides retrodirective system for the control of microwave wireless power transfer," in *2024 SICE International Symposium on Control Systems (SICE ISCS)*, 2024, pp. 99–106.

[4] Q. Yuan, "S-parameters for calculating the maximum efficiency of a mimo-wpt system: Applicable to near/far field coupling, capacitive/magnetic coupling," *IEEE Microwave Magazine*, vol. 24, no. 4, pp. 40–48, 2023.

[5] Q. Hui, K. Jin, and X. Zhu, "Directional radiation technique for maximum receiving power in microwave power transmission system," *IEEE Transactions on Industrial Electronics*, vol. 67, no. 8, pp. 6376–6386, 2020.

[6] T. Matsumuro, Y. Ishikawa, T. Mitani, N. Shinohara, M. Yanagase, and M. Matsunaga, "Study of a single-frequency retrodirective system with a beam pilot signal using dual-mode dielectric resonator antenna elements," *Wireless Power Transfer*, vol. 4, no. 2, p. 132–145, 2017.

[7] A. Hajimiri, B. Abiri, F. Bohn, M. Gal-Katziri, and M. H. Manohara, "Dynamic focusing of large arrays for wireless power transfer and beyond," *IEEE Journal of Solid-State Circuits*, vol. 56, no. 7, pp. 2077–2101, 2021.

[8] T. Matsumuro, Y. Ishikawa, M. Yanagase, and N. Shinohara, "Both-side retrodirective system for minimizing the leak energy in microwave power transmission," in *2018 Asia-Pacific Microwave Conference (APMC)*, 2018, pp. 780–781.

[9] C. D. M. Ambatali and S. Nakasuka, "Controlling the wireless power transfer mechanism of the both-sides retrodirective system," 2024. [Online]. Available: https://arxiv.org/abs/2410.22644

[10] R. Tedrake, *Underactuated Robotics*, 2023. [Online]. Available: https://underactuated.csail.mit.edu

[11] C. Lee, "Fuzzy logic in control systems: fuzzy logic controller. i," *IEEE Transactions on Systems, Man, and Cybernetics*, vol. 20, no. 2, pp. 404–418, 1990.